Illumination from Shadows

Imari Sato, Yoichi Sato, and Katsushi Ikeuchi

Abstract—In this paper, we introduce a method for recovering an illumination distribution of a scene from image brightness inside shadows cast by an object of known shape in the scene. In a natural illumination condition, a scene includes both direct and indirect illumination distributed in a complex way, and it is often difficult to recover an illumination distribution from image brightness observed on an object surface. The main reason for this difficulty is that there is usually not adequate variation in the image brightness observed on the object surface to reflect the subtle characteristics of the entire illumination. In this study, we demonstrate the effectiveness of using occluding information of incoming light in estimating an illumination distribution of a scene. Shadows in a real scene are caused by the occlusion of incoming light, and thus analyzing the relationships between the image brightness and the occlusions of incoming light enables us to reliably estimate an illumination distribution of a scene even in a complex illumination environment. This study further concerns the following two issues that need to be addressed. First, the method combines the illumination analysis with an estimation of the reflectance properties of a shadow surface. This makes the method applicable to the case where reflectance properties of a surface are not known a priori and enlarges the variety of images applicable to the method. Second, we introduce an adaptive sampling framework for efficient estimation of illumination distribution. Using this framework, we are able to avoid unnecessarily dense sampling of the illumination and can estimate the entire illumination distribution more efficiently with a smaller number of sampling directions of the illumination distribution. To demonstrate the effectiveness of the proposed method, we have successfully tested the proposed method by using sets of real images taken in natural illumination conditions with different surface materials of shadow regions.

Keywords—computer vision, physics based vision, illumination distribution estimation

I. INTRODUCTION

The image brightness of a three-dimensional object is the function of the following three components: the distribution of light sources, the shape of a real object; and the reflectance of that real object surface [8], [9]. The relationship among them has provided three major research areas in physics-based vision: shape-from-brightness (with a known reflectance and illumination), reflectance-from-brightness (with a known shape and illumination), and illumination-from-brightness (with a known shape and reflectance).

The first two kinds of analyses, shape-from-brightness and reflectance-from-brightness, have been intensively studied using the shape from shading method [10], [12], [11], [24], as well as through reflectance analysis research [13], [22], [7], [1], [15], [18], [30], [35].

In contrast, relatively limited amounts of research have been conducted in the third area, illumination-from-brightness. This is because real scenes usually include both direct and indirect illumination distributed in a complex way and it is difficult to analyze characteristics of the illumination distribution of the scene from image brightness. Most of the previously proposed approaches were conducted under very specific illumination conditions, e.g., there were several point light sources in the scene, and those approaches were difficult to be extended for more natural illumination conditions [11], [13], [30], [33], [36], or multiple input images taken from different viewing angles were necessary [17], [23].

In this study, we present a method for recovering an illumination distribution of a scene from image brightness observed on an object surface in that scene. To compensate for the insufficient information for the estimation, we propose to use occluding information of incoming light caused by an object in that scene as well as the observed image brightness on an object surface. More specifically, the proposed method recovers the illumination distribution of the scene from image brightness inside shadows cast by an object of known shape in the scene.

Shadows in a real scene are caused by the occlusion of incoming light, and thus contain various pieces of information about the illumination of the scene. However, shadows have been used for determining the 3D shapes and orientations of an object which casts shadows onto the scene [19], [16], [32], [3], while very few studies have focused on the the illuminant information which shadows could provide. In our method, image brightness inside shadows is effectively used for providing distinct clues to estimate an illumination distribution.

The proposed approach estimates an illumination distribution of a scene using the following procedures. The illumination distribution of a scene is first approximated by discrete sampling of an extended light source; whole distribution is represented as a set of point sources equally distributed in the scene. Then this approximation leads each image pixel inside shadows to provide a linear equation with radiance of those light sources as unknowns. Finally, the unknown radiance of each light source is solved from the obtained set of equations. In this paper, we refer to the image with shadows as the *shadow image*, to the object which casts shadows onto the scene as the *occluding object*, and to the surface onto which the *occluding object* casts shadows as the *shadow surface*.

The assumptions that we made for the proposed approach are as follows.

- Known geometry: the 3D shapes of both the *occluding object* and the *occluding surface* are known as well as their relative poses and locations.
- Distant illumination: we assume that light sources in the scene are sufficiently distant from the objects, and thus all light sources project parallel rays onto the object surface. Namely, the distances from the objects to the light sources are not considered in the proposed approach.
- No interreflection: the proposed method does not take into account interreflection between the *shadow surface* and the *occluding object* on the assumption that there is no severe interreflection between them and no multiple scattering of the interreflected rays from them to the scene. As a consequence, objects with darker color and weaker specularity

I. Sato is with Graduate School of Interdisciplinary Information Studies, The University of Tokyo, 7-3-1 Hongo, Bunkyo, Tokyo 113-0033, Japan. E-mail: imarik@iis.u-tokyo.ac.jp .

Y. Sato and K. Ikeuchi are with Institute of Industrial Science, The University of Tokyo, 4-6-1 Komaba, Meguro, Tokyo 153-8505, Japan. E-mail: {ysato, ki}@iis.u-tokyo.ac.jp .

are preferred as *occluding objects* since they do not significantly act as secondary light sources, and the method cannot handle a scene consisting of shiny *occluding objects*.

This study further concerns the following two issues that need to be considered when we tackle this illumination-from-brightness problem. The first issue is how to provide reflectance properties of the *shadow surface* in cases where they are not given a priori. Since it is a common situation that reflectance properties of a surface are not known, a solution to this problem is required to enlarge the variety of images to which the proposed method can be applied. In our approach, instead of assuming any particular reflectance properties of the surface inside shadows, both the illumination distribution of the scene and the reflectance properties of the surface are estimated simultaneously, based on an iterative optimization framework.

The second issue is how to efficiently estimate an illumination distribution of a scene without losing the accuracy of the estimated illumination distribution. To capture the subtle characteristics of the illumination distribution of a scene, the entire distribution must be discretized densely, and this makes the solution exceedingly expensive in terms of processing time and storage requirements. To satisfy both the accuracy and the efficiency claims, we introduce an adaptive sampling framework to sample the illumination distribution of a scene. Using this adaptive sampling framework, we are able to avoid unnecessarily dense sampling of the illumination and estimate overall illumination more efficiently by using fewer sampling directions.

The rest of the paper is organized as follows. We describe how we first obtain a formula which relates an illumination distribution of a scene with the image irradiance of the *shadow image* in Section II and Section III. The formula will later be used as a basis for estimating both the illumination distribution of a real scene and the reflectance properties of the *shadow surface*. Using this formula, we explain how to estimate an illumination radiance distribution from the observed image irradiance of a *shadow image* in Section IV. In this section, we consider the following two cases separately: (1) where the reflectance properties of the *shadow surface* are known, (2) where those properties are not known. We also introduce an adaptive sampling framework for efficient approximation of the entire illumination, and show experimental results of the proposed method applied to images taken in natural illumination conditions in Section V. Finally, we discuss some of the related work proposed in the field of computer graphics in Section VI, and present concluding remarks and future research directions in Section VII. This paper is an expanded and more detailed version of the works we presented in [27], [28].

II. RELATING ILLUMINATION RADIANCE WITH IMAGE IRRADIANCE

In this section, we describe how we obtain a formula which relates an illumination distribution of a real scene with the image irradiance of a *shadow image*. The formula will later be used as a basis for estimating the illumination distribution of a scene and the reflectance properties of a *shadow surface*.

First, we find a relationship between the illumination distribution of a real scene and the irradiance at a surface point in
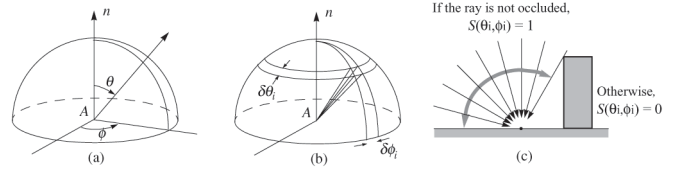

Fig. 1. (a) the direction of incident and emitted light rays (b) infinitesimal patch of an extended light source, (c) occlusion of incoming light

the scene. [1] To take illumination from all directions into account, let us consider an infinitesimal patch of the extended light source, of a size $\delta\theta_i$ in polar angle and $\delta\phi_i$ in azimuth as shown in Fig. 1.

Seen from the center point A, this patch subtends a solid angle $\delta\omega = sin\theta_i\delta\theta_i\delta\phi_i$. Let $L_0(\theta_i, \phi_i)$ be the illumination radiance per unit solid angle coming from the direction (θ_i, ϕ_i); then the radiance from the patch is $L_0(\theta_i, \phi_i)sin\theta_i\delta\theta_i\delta\phi_i$, and the total irradiance of the surface point A is [9]

$$E = \int_{-\pi}^{\pi} \int_{0}^{\frac{\pi}{2}} L_0(\theta_i, \phi_i)cos\theta_i sin\theta_i d\theta_i d\phi_i \qquad (1)$$

Then occlusion of the incoming light by the *occluding object* is considered as

$$E = \int_{-\pi}^{\pi} \int_{0}^{\frac{\pi}{2}} L_0(\theta_i, \phi_i)S(\theta_i, \phi_i)cos\theta_i sin\theta_i d\theta_i d\phi_i \qquad (2)$$

where $S(\theta_i, \phi_i)$ are occlusion coefficients; $S(\theta_i, \phi_i) = 0$ if $L_0(\theta_i, \phi_i)$ is occluded by the *occluding object*; Otherwise $S(\theta_i, \phi_i) = 1$ (Fig. 1 (c)).

Some of the incoming light at point A is reflected toward the image plane. As a result, point A becomes a secondary light source with scene radiance.

The bidirectional reflectance distribution function (BRDF) $f(\theta_i, \phi_i; \theta_e, \phi_e)$ is defined as a ratio of the radiance of a surface as viewed from the direction (θ_e, ϕ_e) to the irradiance resulting from illumination from the direction (θ_i, ϕ_i). Thus, by integrating the product of the BRDF and the illumination radiance over the entire hemisphere, the scene radiance $Rs(\theta_e, \phi_e)$ viewed from the direction (θ_e, ϕ_e) is computed as

$$Rs(\theta_e, \phi_e) = \int_{-\pi}^{\pi} \int_{0}^{\frac{\pi}{2}} f(\theta_i, \phi_i; \theta_e, \phi_e)L_0(\theta_i, \phi_i)$$
$$S(\theta_i, \phi_i)cos\theta_i sin\theta_i d\theta_i d\phi_i \qquad (3)$$

Finally, the illumination radiance of the scene is related with image irradiance on the image plane. Since what we actually observe is not image irradiance on the image plane, but rather a recorded pixel value in a *shadow image*, it is necessary to consider the conversion of the image irradiance into a pixel value of a corresponding point in the image. This conversion includes

---

[1] For a good reference of the radiometric properties of light in a space, see [21].

several factors such as D/A and A/D conversions in a CCD camera and a frame grabber.

Other studies concluded that image irradiance was proportional to scene radiance [9]. In our work, we calibrate a linearity of the CCD camera by using a Macbeth color chart with known reflectivity so that the recorded pixel values also become proportional to the scene radiance of the surface. From (3) the pixel value of the *shadow image* $P(\theta_e, \phi_e)$ is thus computed as

$$P(\theta_e, \phi_e) = k \int_{-\pi}^{\pi} \int_{0}^{\frac{\pi}{2}} f(\theta_i, \phi_i; \theta_e, \phi_e) L_0(\theta_i, \phi_i)$$
$$S(\theta_i, \phi_i) cos\theta_i sin\theta_i d\theta_i d\phi_i \qquad (4)$$

where k is a scaling factor between scene radiance and a pixel value. Due to the scaling factor k, we are able to estimate unknown $L_0(\theta_i, \phi_i)(i = 1, 2, \cdots, n)$ up to scale. To obtain the scale factor k, we need to perform photometric calibration between pixel intensity and the physical unit $(watt/m^2)$ for the irradiance.

III. APPROXIMATION OF ILLUMINATION DISTRIBUTION WITH DISCRETE SAMPLING

In our implementation of the proposed method, to solve for the unknown radiance $L_0(\theta_i, \phi_i)$ which is continuously distributed on the surface of the extended light source from the recorded pixel values of the *shadow surface*, the illumination distribution is approximated by discrete sampling of radiance over the entire surface of the extended light source. This can be considered as representing the illumination distribution of the scene by using a collection of light sources with an equal solid angle. As a result, the double integral in (4) is approximated as

$$P(\theta_e, \phi_e) = \sum_{i=1}^{n} f(\theta_i, \phi_i; \theta_e, \phi_e) L(\theta_i, \phi_i) S(\theta_i, \phi_i) cos\theta_i \omega_i$$
$$(5)$$

where n is the number of sampling directions, $L(\theta_i, \phi_i)$ is the illumination radiance per unit solid angle coming from the direction (θ_i, ϕ_i), which also includes the scaling factor k between scene radiance and a pixel value, and ω_i is a solid angle for the sampling direction (θ_i, ϕ_i).

For instance, node directions of a geodesic dome can be used for uniform sampling of the illumination distribution. By using n nodes of a geodesic dome in a northern hemisphere as a sampling direction, the illumination distribution of the scene is approximated as a collection of directional light sources distributed with an equal solid angle $\omega = 2\pi/n$.

IV. ESTIMATION OF RADIANCE DISTRIBUTION BASED ON REFLECTANCE PROPERTIES OF SHADOW SURFACE

After obtaining the formula that relates the illumination radiance of the scene with the pixel values of the *shadow image*, illumination radiance is estimated based on the recorded pixel values of the *shadow image*.

In (5), the recorded pixel value $P(\theta_e, \phi_e)$ is computed as a function of the illumination radiance $L(\theta_i, \phi_i)$ and the BRDF $f(\theta_i, \phi_i; \theta_e, \phi_i)$. Accordingly, in the following sections, we take different approaches, depending on whether BRDF of the surface is given.
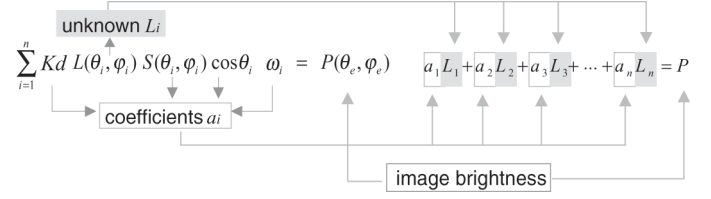

Fig. 2. Each pixel provides a linear equation.

A. Known Reflectance Properties

A.1 Lambertian

Let us start with the simplest case where the *shadow surface* is a Lambertian surface whose reflectance properties are given.

BRDF $f(\theta_i, \phi_i; \theta_e, \phi_e)$ for a Lambertian surface is known to be a constant. From (5), an equation for a Lambertian surface is obtained as

$$P(\theta_e, \phi_e) = \sum_{i=1}^{n} K_d L(\theta_i, \phi_i) S(\theta_i, \phi_i) cos\theta_i \omega_i \qquad (6)$$

where K_d is a diffuse reflection parameter of the surface.

From (6), the recorded pixel value P for an image pixel is given as

$$P = \sum_{i=1}^{n} a_i L_i \qquad (7)$$

where L_i $(i = 1, 2, \cdots, n)$ are n unknown illumination radiance specified by n node directions of a geodesic dome. As shown in Fig. 2, the coefficients $a_i (i = 1, 2, \cdots, n)$ represent $K_d S(\theta_i, \phi_i) \cos\theta_i \omega_i$ in (6); we can compute these coefficients from the 3D geometry of a surface point, the *occluding object* and the illuminant direction. In our examples, we use a modeling tool called the 3D Builder from 3D Construction Company [37] to recover the shape of an *occluding object* and also the camera parameters from a *shadow image*. At the same time, the plane of $z = 0$ is defined on the *shadow surface*. [2]

If we select a number of pixels, say m pixels, a set of linear equations is obtained as

$$P_j = \sum_{i=1}^{n} a_{ji} L_i \qquad (j = 1, 2, \cdots, m) \qquad (8)$$

Therefore, by selecting a sufficiently large number of image pixels, we are able to solve for a solution set of unknown L_i's. [3] For our current implementation, we solve the problem by using the linear least square algorithm with non-negativity constraints (using a standard MATLAB function) to obtain an optimal solution with no negative components.

---

[2] It is worth noting that, as long as the 3D shape of the *shadow surface* is provided in some manner, e.g., by using a range sensor, the *shadow surface* need not be a planar surface. It is rather reasonable to think that a curved *shadow surface* has the potential for providing more variation in a_{ji} in (8) than an ordinary planar surface would since $cos\theta_i$ term of a_i in (7) also slightly changes from image pixel to pixel. Unless severe interreflection occurs within the surface, our method can be applied to a curved *shadow surface*.

[3] More details of the pixel selection are found in the Appendix.

It should be noted that each pixel $P(\theta_e, \phi_e)$ consists of 3 color bands (R, G, and B) and likewise the diffuse parameter K_d consists of 3 parameters $(K_{d,R}, K_{d,G}, K_{d,B})$. Each color band of $L(\theta_i, \phi_i)$ is thus estimated separately from the corresponding band of the image pixel and that of the diffuse parameter K_d. For the sake of simplicity in our discussion, we explain the proposed method by using $L(\theta_i, \phi_i)$, $P(\theta_e, \phi_e)$, K_d and do not refer to each of their color bands in the following sections.

We must also draw attention to the importance of shadow coefficients for recovering illumination distribution of a scene from the observed brightness on an object surface. For instance, consider the case described above where the given *shadow surface* is a Lambertian surface. If we do not take into account the occlusion of including light, the variation of a_{ji} in (8) is caused only by the cosine factor of incoming light direction and the surface normal direction of the corresponding point on the *shadow surface* ($cos\theta_{ji}$). As a result, the estimation of illumination distribution by solving the equation (8) for a solution set of unknown L_i's tends to become numerically unstable.

In contrast, taking into account the occlusion of incoming light tells us that the variation of a_{ji} becomes much larger since the shadow coefficient $S(\theta_i, \phi_i)$ in (6) changes significantly, i.e., either 0 or 1, from point to point on the *shadow surface* depending on the spatial relationships among the location of the point, the *occluding object*, and the sampling direction of the illumination distribution, as is well illustrated in Lambert's work described in [5]. This characteristics of shadows enables us to reliably recover the illumination distribution of the scene from brightness changes inside shadows.

A.2 Non-Lambertian surface

The proposed approach may be extended to other reflection models as well. The only condition for a model to satisfy is that it enables us to analytically solve for a solution set of unknown illumination radiance from image brightness.

Take a simplified Torrance-Sparrow reflection model [22], [34] for example; the pixel value of a *shadow image* $P(\theta_e, \phi_e)$ is computed as

$$
\begin{aligned}
P(\theta_e, \phi_e) = & \sum_{i=1}^{n} K_d L(\theta_i, \phi_i) S(\theta_i, \phi_i) cos\theta_i \omega_i + \\
& \sum_{i=1}^{n} K_s L(\theta_i, \phi_i) S(\theta_i, \phi_i) \omega_i \frac{1}{cos\theta_e} e^{\frac{-\gamma(\theta_i, \phi_i)^2}{2\sigma^2}} \\
= & \sum_{i=1}^{n} (K_d cos\theta_i + K_s \frac{1}{cos\theta_e} e^{\frac{-\gamma(\theta_i, \phi_i)^2}{2\sigma^2}}) \\
& S(\theta_i, \phi_i) \omega_i L(\theta_i, \phi_i) \quad\quad (9)
\end{aligned}
$$

where $\gamma(\theta_i, \phi_i)$ is the angle between the surface normal and the bisector of the light source direction and the viewing direction, K_d and K_s are constants for the diffuse and specular reflection components, and σ is the standard deviation of a facet slope of the Torrance-Sparrow reflection model.

From (9), we obtain a linear equation for each image pixel where $L(\theta_i, \phi_i)(i = 1, 2, \cdots, n)$ are unknown illumination radiance, and $(K_d cos\theta_i + K_s \frac{1}{cos\theta_e} e^{\frac{-\gamma(\theta_i, \phi_i)^2}{2\sigma^2}}) S(\theta_i, \phi_i) \omega_i$ ($i = 1, 2, \cdots, n$) are known coefficients.

Again, if we use a sufficiently large number of pixels for the estimation, we are able to solve for a solution set of unknown illumination radiance $L(\theta_i, \phi_i)(i = 1, 2, \cdots, n)$ in this case.

A.3 Experimental Results for Known Lambertian Surface

We have tested the proposed approach using an image with an *occluding object*, i.e., *shadow image*, taken under usual illumination environmental conditions, including direct light sources such as fluorescent lamps, as well as indirect illumination such as reflections from a ceiling and a wall (Fig. 3 (b)).

First, an illumination distribution of the scene was estimated using the image irradiance inside shadows in the *shadow image*. Then a synthetic object with the same shape as that of the *occluding object* was superimposed onto an image of the scene taken without the *occluding object*, which is referred as a *surface image*, using the rendering method described in [29]. Note that our algorithm does not require this *surface image* in the process of illumination estimation in the case where the reflectance properties of the *shadow surface* are given. This *surface image* is used here as a background image for superimposing the synthetic *occluding object* onto the scene.

Synthesized results are shown in Fig. 4 (a), (b), and (c). Also, we superimposed another synthetic object of a different shape onto the scene in Fig. 4 (d). The number of nodes of a geodesic dome used for the estimation is shown under the resulting image.

As we see in Fig. 4, the larger the number of nodes we used, the more the shadows of the synthetic object resembled those of the *occluding object* in the *shadow image*. Especially in the case of 520 nodes, the shadows of the synthetic object are nearly indistinguishable from those of the *occluding object* in the *shadow image*; this shows that the estimated illumination distribution gives a good presentation of that of the real scene. [4]

Fig. 5 numerically shows the improvement of the accuracy obtained by increasing the number of samplings. Here, the estimated illumination distribution was evaluated in a different scene condition where the *occluding object* was rotated 45 degrees on its z axis. The vertical axis represents the average error in pixel values (0 to 255) inside the shadow regions in the synthesized images compared with those in the *shadow image*. The horizontal axis represents the number of nodes of a geodesic dome used for the estimation. The small pictures right next to the plot show error distributions inside shadow regions in the synthesized images. Darker color represents larger error in a pixel value. The average error at the zero sampling of illumination radiance represents, for reference, the average pixel value inside the shadow regions of the *shadow image*.

In this plot, we see that flattening of the error curve before convergence to the exact solutions occurs. This is likely caused by the following factors. The first of these is the errors in the measurements of the 3D shapes of the *occluding object* and the *shadow surface*. The second factor is the errors in the given reflectance properties of the *shadow surface*; there is some possibility that the *shadow surface* is not a perfect Lambertian surface. The third factor is related to our lighting model that approximates the illumination distribution of a scene by discrete sampling of an extended light source on the assumption that

---

[4]We see some "stair-casting" artifacts inside the synthesized shadows that result from our approximation of continuous illumination distribution by discrete sampling of its radiance. One approach to reduce this artifact is to increase the number of point light sources used for rendering, whose radiance is given by interpolating the estimated radiance L_i of the neighboring light sources.

(a)   (b)
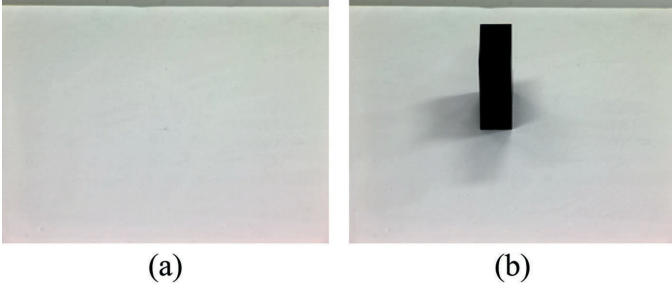
Fig. 3. Input images : (a) *surface image* (b) *shadow image*
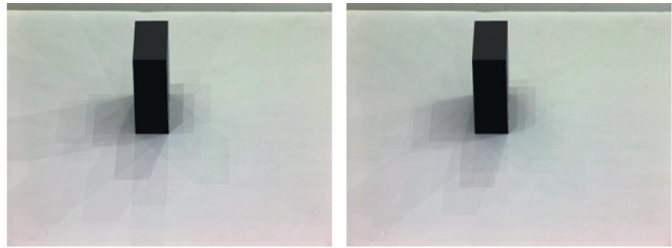
(a) number of samplings : 90   (b) number of samplings : 190
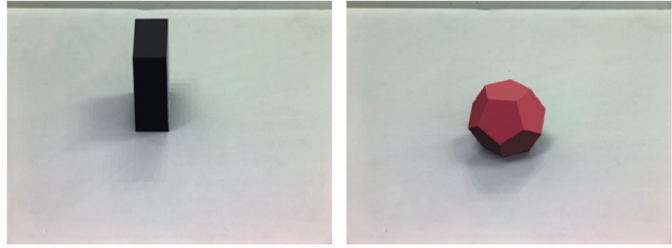
(c) number of samplings : 520   (d) number of samplings : 520

Fig. 4. Synthesized images: known reflectance property

light sources in the scene are sufficiently distant from the objects. The input image used in this experiment was taken in an indoor environment, this assumption might not perfectly hold. The last factor concerns our assumption that there is no interreflection between the *occluding object* and the *shadow surface*.

B. Unknown Reflectance Properties

B.1 Uniform Surface Material

There certainly may be a situation where reflectance properties of a surface are not known a priori, and we need to somehow provide those properties in advance. To cope with this situation, we combine the illumination analysis with an estimation of the reflectance properties of the *shadow surface*. More specifically, we estimate both the illumination distribution of the scene and the reflectance properties of the surface simultaneously, based on an iterative optimization framework. We will later explain details of this iterative optimization framework in conjunction with the adaptive sampling method described in SectionV. This approach is based on the assumption that the *shadow surface* has uniform reflectance properties over the entire surface.
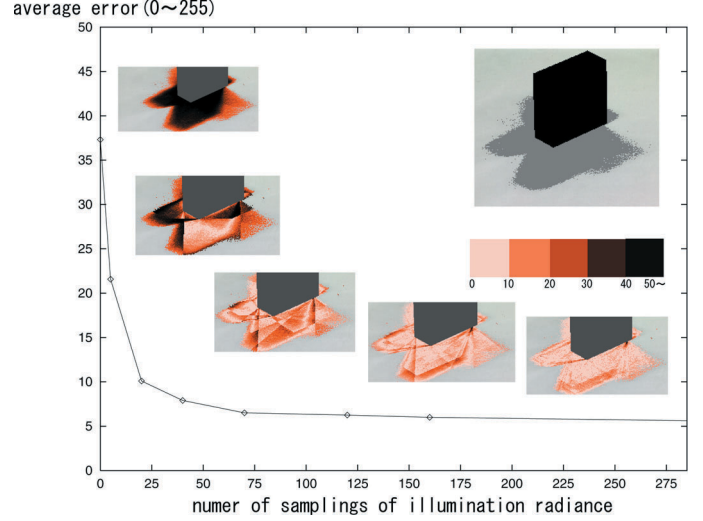

Fig. 5. Error Analysis: The vertical axis represents the average error in pixel values (0 to 255) inside the shadow regions in the synthesized images compared with those in the *shadow image*. The horizontal axis represents the number of nodes of a geodesic dome used for the estimation. The small pictures right next to the plot show error distributions inside shadow regions in the synthesized images. Darker color represents larger error in a pixel value.

B.2 Non-Uniform Surface Material

The last case is where the BRDF is not given, and the *shadow surface* does not have uniform reflectance properties, e.g., surfaces with some textures. Even in this case, we are still able to estimate an illumination distribution of a scene from shadows if it is conceivable that the *shadow surface* is a Lambertian surface.

The question we have to consider here is how to cancel the additional unknown number K_d in (6). An additional image of the scene taken without the *occluding object*, called the *surface image*, is used for this purpose. The image irradiance of a *surface image* represents the surface color in the case where none of the incoming light is occluded. Accordingly, in the case of the *surface image*, the shadow coefficients $S(\theta_i, \phi_i)$ always become $S(\theta_i, \phi_i) = 1$. Therefore, the image irradiance $P'(\theta_e, \phi_e)$ of the *surface image* is computed from (6) as

$$P'(\theta_e, \phi_e) = K_d \sum_{j=1}^{n} L(\theta_j, \phi_j) cos\theta_j \omega_j \qquad (10)$$

From (6) and (10), the unknown K_d is canceled.

$$\frac{P(\theta_e, \phi_e)}{P'(\theta_e, \phi_e)} = \frac{K_d \sum_{i=1}^{n} L(\theta_i, \phi_i) cos\theta_i S(\theta_i, \phi_i) \omega_i}{K_d \sum_{j=1}^{n} L(\theta_j, \phi_j) cos\theta_j \omega_j}$$

$$= \sum_{i=1}^{n} \frac{L(\theta_i, \phi_i)}{\sum_{j=1}^{n} L(\theta_j, \phi_j) cos\theta_j \omega_j} cos\theta_i S(\theta_i, \phi_i) \omega_i \qquad (11)$$

Finally, we obtain a linear equation for each image pixel where $\frac{L(\theta_i, \phi_i)}{\sum_{j=1}^{n} L(\theta_j, \phi_j) cos\theta_j \omega_j}$ are unknowns, $cos\theta_i S(\theta_i, \phi_i) \omega_i$ are computable coefficients, and $\frac{P(\theta_e, \phi_e)}{P'(\theta_e, \phi_e)}$ is a right-hand side quantity. Again, if we use a sufficiently large number of pixels for the
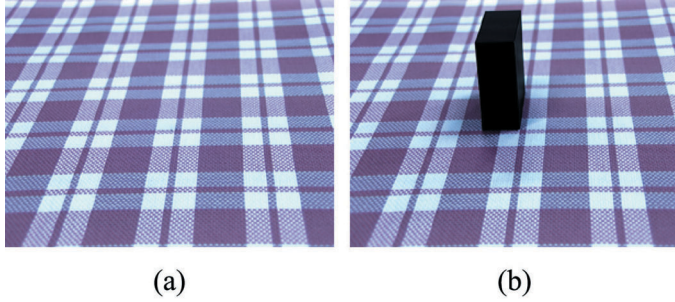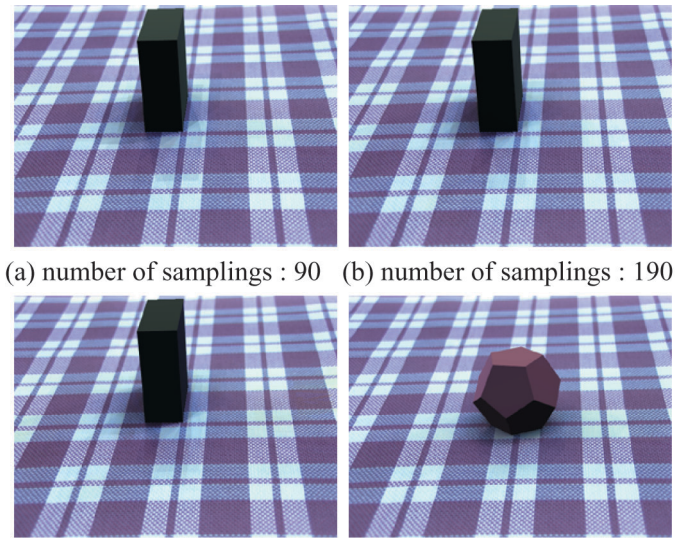
(a)   (b)

Fig. 6. Input images : (a) *surface image* (b) *shadow image*

(a) number of samplings : 90   (b) number of samplings : 190

(c) number of samplings : 520 (d) number of samplings : 520

Fig. 7. Synthesized images: unknown reflectance property

Fig. 8. Error Analysis: unknown reflectance property

estimation, we are able to solve the set of linear equations for a solution set of unknown $\frac{L(\theta_i, \phi_i)}{\sum_{j=1}^{n} L(\theta_j, \phi_j) cos\theta_j}$ $(i = 1, 2, \cdots, n)$.

We should point out that the estimated radiance from these equations is a ratio of the illumination radiance in one direction $L(\theta_i, \phi_i)$ to scene irradiance at the surface point $\sum_{j=1}^{n} L(\theta_j, \phi_j) cos\theta_j \omega_j$. As a result, we cannot relate the estimated radiance over the color bands unless the ratio of the scene irradiance among color bands is provided. It is, however, not so difficult to obtain this ratio. For instance, if there is a surface with a white color in the scene, the recorded color of the surface directly indicates the ratio of the scene irradiance among color bands. Otherwise, an assumption regarding total radiance is required.

B.3 Experimental Results for Non-Uniform Surface Material

The input images used in this experiment are shown in Fig. 6. The illumination distribution of the scene was estimated using the image irradiance of both the *shadow image* and the *surface image*, and a synthetic *occluding object* was superimposed onto the *surface image* using the estimated illumination distribution. Synthesized results are shown in Fig. 7. Again, in the case of 520 nodes, the shadows in the resulting image resemble those of
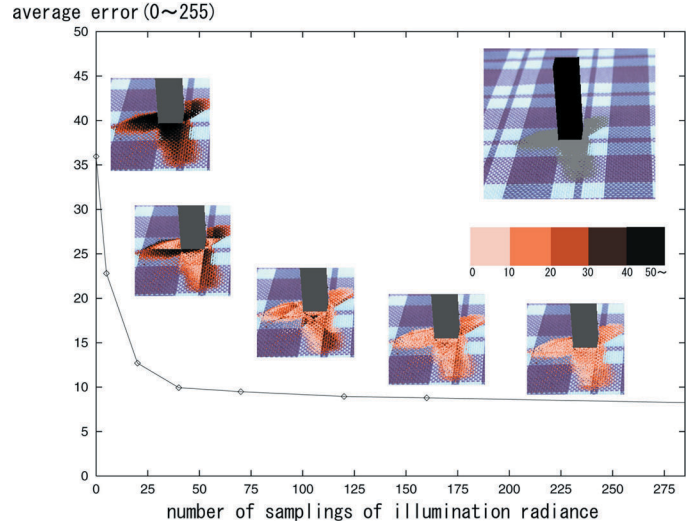
the *occluding object* in the *shadow image*. This shows that the estimated illumination distribution gives a good representation of the characteristics of the real scene.

Fig. 8 numerically shows the improvement of the accuracy by increasing the number of samplings. The estimated illumination distribution was evaluated using a new *occluding object* with a different shape. From the plot in the figure, we can clearly see that the accuracy improves as we use more sampling directions of the illumination distribution. It is likely that the flattening of the error curve before convergence to the exact solutions is caused by the same factors described in Section IV-A.3.

V. ADAPTIVE ESTIMATION OF ILLUMINATION DISTRIBUTION WITH UNKNOWN REFLECTANCE PROPERTIES OF SHADOW SURFACE

This section further concerns the following two issues that further generalize the proposed approach. The first issue is how to provide reflectance properties of a surface inside shadows in cases where they are not given a priori, and the *shadow surface* is not conceivable as a Lambertian surface.

The second issue is how to efficiently estimate an illumination distribution of a scene without losing the accuracy of the estimated illumination distribution. In Section IV, we have estimated an illumination distribution of a real scene by sampling the distribution at an equal solid angle given as node directions of a geodesic dome. For more efficiently estimating the illumination distribution of a scene using fewer sampling directions of illumination radiance, we propose to increase sampling directions adaptively based on the estimation at the previous iteration, rather than by using a uniform discretization of the overall illumination distribution in this section.

A. Basic Steps of the Proposed Approach

To take both diffuse and specular reflections of the *shadow surface* into consideration, a simplified Torrance-Sparrow reflection model (9) described in Section IV-A.2 is reused. Based on this reflection model, both the illumination distribution of the

scene and the reflectance properties of the *shadow surface* are estimated from image brightness inside shadows as described in the following steps.

1. Initialize the reflectance parameters of the *shadow surface*. Typically, we assume the *shadow surface* to be Lambertian, and the diffuse parameter K_d is set to be the pixel value of the brightest point on the *shadow surface*. The specular parameters are set to be zero ($K_s = 0, \sigma = 0$). [5]

2. Select image pixels whose brightness is used for estimating both the illumination distribution of a scene and the reflectance properties of the *shadow surface*. This selection is done by examining the coefficients a_i in (7) in the manner described in the Appendix.

3. Estimate illumination radiance $L(\theta_i, \phi_i)$. Using the reflectance parameters (K_d, K_s, σ) and image brightness inside shadows in the *shadow image*, the radiance distribution $L(\theta_i, \phi_i)$ is estimated as described in Section IV-A.2.

4. Estimate the reflectance parameters of the *shadow surface* (K_d, K_s, σ) from the obtained radiance distribution of the scene $L(\theta_i, \phi_i)$ by using an optimization technique. (Section V-B)

5. Proceed to the next step if there is no significant change in the estimated values $L(\theta_i, \phi_i), K_d, K_s$, and σ. Otherwise, go back to Step 3. By estimating both the radiance distribution of the scene and the reflectance parameters of the *shadow surface* iteratively, we can obtain the best estimation of those values for a given set of sampling directions of the illumination radiance distribution of the scene.

6. Terminate the estimation process if the obtained illumination radiance distribution approximates the real radiance distribution with sufficient accuracy. Otherwise, proceed to the next step.

7. Increase the sampling directions of the illumination distribution adaptively based on the obtained illumination radiance distribution $L(\theta_i, \phi_i)$. (Section V-C)

   Then go back to Step 2.

In the following sections, each step of the proposed approach will be explained in more detail.

B. Estimation of Reflectance Parameters of Shadow Surface based on Radiance Distribution

In this section, we describe how to estimate the reflectance parameters of the *shadow surface* (K_d, K_s, σ) by using the estimated radiance distribution of the scene $L(\theta_i, \phi_i)$.

Unlike the estimation of the radiance distribution of the scene $L(\theta_i, \phi_i)$, which can be done by solving a set of linear equations, we estimate the reflectance parameters of the *shadow surface* by minimizing the sum of the squared difference between the observed pixel intensities in the *shadow image* and the pixel values computed for the corresponding surface points. Hence, the function to be minimized is defined as

$$f = \sum_{j=1}^{m} (P_j' - P_j)^2 \tag{12}$$

where P_j' is the observed pixel intensity in shadows cast by the *occluding object*, P_j is the pixel value of the corresponding surface points computed by using the given radiance distribution of the scene $L(\theta_i, \phi_i)$ in (9), m is the number of pixels used for minimization. In our method, the error function in (12) is minimized with respect to the reflectance parameters K_d, K_s, and σ by the Powell method to obtain the best estimation of those reflectance parameters [25]. As has been noted, this approach is based on the assumption that the *shadow surface* has uniform reflectance properties over the entire surface.

C. Adaptive Sampling of Radiance Distribution

If the estimated radiance distribution for a set of sampling directions does not approximate the illumination distribution of the scene with sufficient accuracy, we increase the sampling directions adaptively based on the current estimation of the illumination radiance distribution.

Radiance distribution changes very rapidly around a direct light source such as a fluorescent light. Therefore, the radiance distribution has to be approximated by using a large number of samplings so that the rapid change of radiance distribution around the direct light source is captured. Also, to correctly reproduce soft shadows cast by extended light sources, radiance distribution inside a direct light source has to be sampled densely.

On the other hand, coarse sampling of radiance distribution is enough for an indirect light source such as a wall whose amount of radiance remains small. As a result, the number of sampling directions required for accurately estimating an illumination distribution of a real scene becomes exceedingly large.

To overcome this problem, we increase sampling directions adaptively based on the estimation at the previous iteration, rather than by using a uniform discretization of the overall illumination distribution. In particular, we increase sampling directions around and within direct light sources. [6]

Based on the estimated radiance distribution $L(\theta_i, \phi_i)$ for the sampling directions at the previous step, additional sampling directions are determined as follows.

Suppose three sampling directions with radiance values L_1, L_2, and L_3 are placed to form a triangle M_1 as illustrated in Fig. 9. To determine whether a new sampling direction needs to be added between L_1 and L_2, we consider the following cost function.
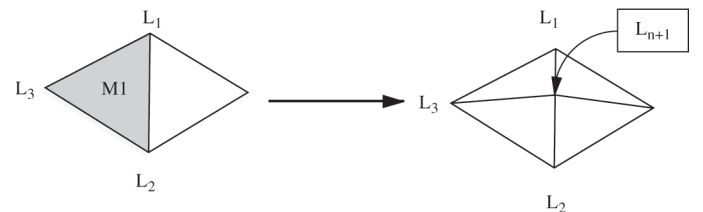

Fig. 9. Subdivision of sampling directions

---

[5]Note that the initial value of K_d is not so important since there is a scaling factor between the reflectance parameters and illumination radiance values in any case. To fix the scaling factor, we need to perform photometric calibration of our imaging system with a calibration target whose reflectance is given a priori.

[6]A similar sampling method has been employed in radiosity computation to efficiently simulate the brightness distribution of a room [4].

$$U(L_1, L_2) = diff(L_1, L_2) + \alpha min(L_1, L_2) angle(L_1, L_2) \tag{13}$$

where $diff(L_1, L_2)$ is the radiance difference between L_1 and L_2, $min(L_1, L_2)$ gives the smaller radiance of L_1 and L_2, $angle(L_1, L_2)$ is the angle between directions to L_1 and L_2, and α is the manually specified parameter which determines the relative weights of those two factors. The first term is required to capture the rapid change of radiance distribution around direct light sources, while the second term leads to fine sampling of the radiance distribution inside direct light sources. The additional term $angle(L_1, L_2)$ is used for avoiding unnecessarily dense sampling inside direct light sources. In our experiments, α is set to 0.5.

If the cost U is large, a new sampling direction is added between L_1 and L_2. In our experiments, we computed the cost function values U for all pairs of neighboring sampling directions, then added additional sampling directions for the first 50% of all the pairs in the order of the cost function values U.

D. Experimental Results for Adaptive Sampling Method

We have tested the proposed adaptive sampling method by using real images taken in both indoor and outdoor environments. In the following experiment, the adaptive sampling technique was applied to a uniform unknown reflectance properties case. The *shadow image* shown in Fig. 10 was used here as an input of a indoor scene.

Starting from a small number of uniform sampling directions of the illumination distribution, the estimation of the radiance distribution of the scene was iteratively refined. At the same time, the reflectance parameters (K_d, K_s, and σ) of the *shadow surface* were estimated as explained in Section V-B. Then an appearance of the *shadow surface* around the *occluding object* was synthesized using the estimated radiance distribution of the scene and the estimated reflectance parameters of the *shadow surface*.

The region inside the red rectangle in Fig. 10 (b) was replaced with the synthesized appearances in the left column in Fig. 11. The number of sampling directions of the radiance distribution used for the estimation is shown under the resulting images. Here, the resulting shadows of the synthetic occluding object resemble more closely those of the *occluding object* in the *shadow image* as we increase the number of sampling directions based on the proposed adaptive sampling technique. Finally, in the case of 140 sampling directions, the synthesized shadows of the *occluding object* blend into the input *shadow image* well, and few distinct boundaries in the shadows are seen in the resulting composite image.

To see how well the adaptive sampling of radiance distribution works in this example, we took an omni-directional image of the office scene as a ground truth. The middle column of Fig. 11 shows the omni-directional image of the scene taken by placing a camera with a fisheye lens looking upward on the *shadow surface* in Fig. 10 (a). The omni-directional image shows both direct light sources, i.e., the fluorescent lamps in our office, and indirect light sources such as the ceiling and

(a)   (b)
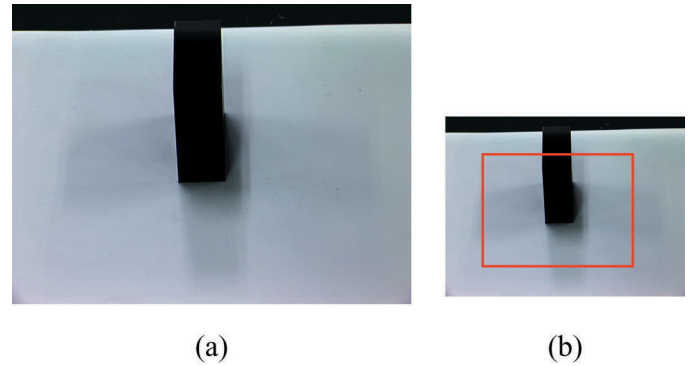
Fig. 10. Input image : (a) *shadow image* taken of an indoor scene (b) the region which synthesized images with the estimated radiance distribution and reflectance parameters are superimposed.

n = 20

n = 40

n = 80

(a)   (b)   (c)
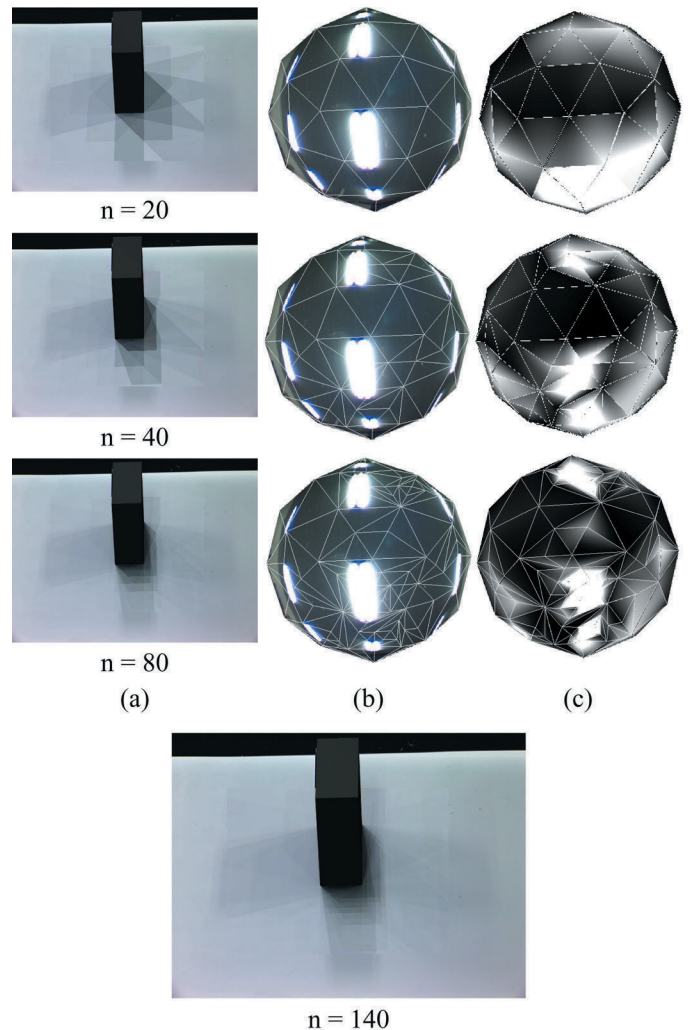
n = 140

Fig. 11. Adaptive refinement of illumination distribution estimation: (a) synthesized images with the estimated radiance distribution and reflectance parameters (b) adaptive refinement of sampling directions with a ground truth of an omni-directional image of the scene (c) the estimated radiance values visualized for comparison with the ground truth
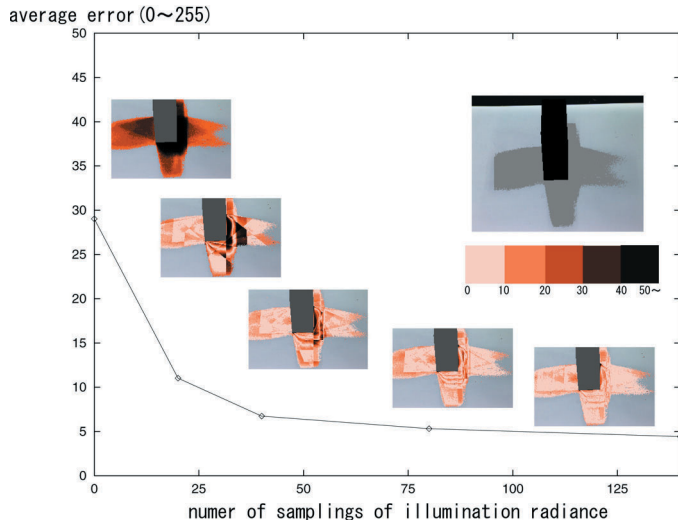
average error (0~255)

number of samplings of illumination radiance

Fig. 12. Error Analysis
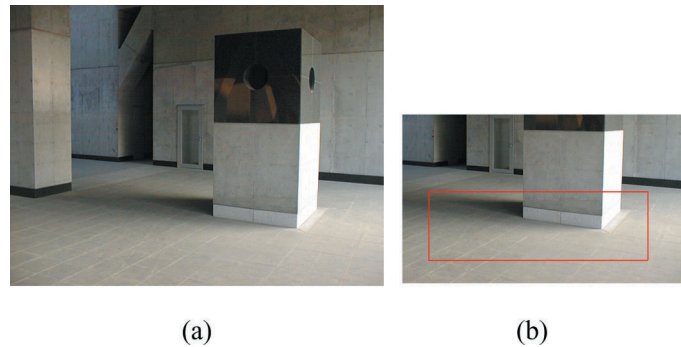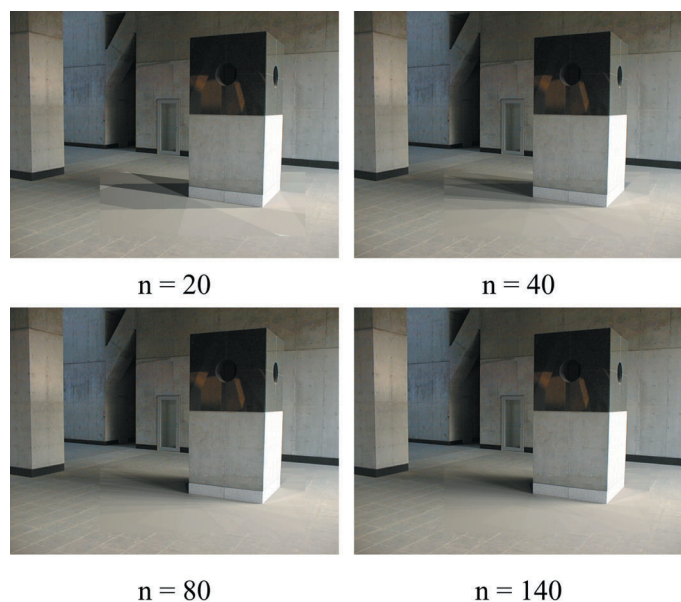

(a)															(b)

Fig. 13. Input image : (a) *shadow image* taken in an outdoor scene (b) the region where synthesized images with the estimated radiance distribution and reflectance parameters are superimposed in Figure 14

n = 20															n = 40

n = 80															n = 140

Fig. 14. Adaptive refinement of illumination distribution estimation: synthesized images with the estimated radiance distribution and reflectance parameters

walls. The right column of Fig. 11 shows the estimated radiance values visualized for comparison with the ground truth. In those images in Fig. 11 (b) and (c), we can see that sampling directions of the radiance distribution were nicely added only around the direct light sources at each step by the proposed adaptive sampling framework, starting from the coarse sampling directions at the top row.

Fig. 12 numerically shows the improvement of the accuracy by adaptive refinement of sampling directions and the estimation of reflectance properties of the *shadow surface*. From the plot in the figure, we can clearly see that the accuracy improves rapidly as we adaptively increase the sampling directions of the radiance distribution.

To confirm the merit of the adaptive sampling framework, we also estimated the illumination radiance distribution with uniform sampling. In that case, even 300 uniformly sampled directions could not achieve the same level of accuracy as the estimation result obtained by 80 sampling directions with the proposed framework.

Fig. 13 (a) shows another example image taken outside the entrance lobby of our building in the late afternoon. In this image, we used the rectangular pole with two colors as an *occluding object* casting shadows. In the same way as the previous example, an appearance of the *shadow surface* around the *occluding object*, illustrated with a red rectangle in Fig. 13 (b), was synthesized by using the estimated radiance distribution of the scene and the estimated reflectance parameters of the *shadow surface*. Fig. 14 shows the resulting images obtained by the use of our method. Although the grid pattern on the *shadow surface* is missing in those synthesized images due to the assumption of uniform reflectance on the *shadow image*, the appearance of the shadow around the *occluding objects* is virtually indistinguishable in the case of 140 sampling directions. This shows that the estimated illumination distribution well represents the characteristics of the real scene.

VI. DISCUSSION

In the field of computer graphics, there have also been several methods proposed for recovering an illumination distribution of a real scene from appearance changes observed on object surfaces in the scene. Most of them have been conducted in fully computer-generated environments where a designer specified the geometry and reflectance of whole scenes and the locations of all light sources [31], [14]; those methods were mainly developed for assisting designers in achieving desirable effects such as highlights and shadows in the synthesized image.

Some researchers extended similar approaches for real images and estimated radiance of real light sources in the scene. Fournier et al. [6] estimated radiance of the light sources with users' defined fix locations on the assumption that all surfaces were Lambertian surfaces. Later, Marschner and Greenberg [20] introduced to approximate the entire illumination with a set of basis lights located in the scene. Although this method has an advantage over the previous methods of not requiring knowl-

edge about the light locations of the scene, the estimation depends entirely on the appearance changes observed on an object surface assumed to be Lambertian, and therefore some restrictions are imposed on the shape of the object, e.g., the object must have a large amount of curvature. Recently, Ramamoorthi and Hanrahan [26] introduced a signal-processing framework that described the reflected light field as a convolution of the lighting and BRDF, and showed under which condition lighting and BRDF recovery could be done robustly. Simultaneously, Basri and Jacobs [2] reported that the images of a convex Lambertian object obtained under a wide variety of lighting conditions could be approximated with a low-dimensional linear subspace by using a similar signal-processing approach.

We are currently investigating the analysis of the problem of illumination estimation from shadows in their signal-processing framework. It was found through our preliminary experiments that high frequency components of the appearance of an object surface could retain significant energy by taking the shadow coefficients on the object surface as well as its BRDF into account. This indicates that the use of shadows for the illumination estimation has the significant advantage of providing more clues to the high frequency components of illumination distribution of a scene.

VII. Conclusions

In this study, we have presented a method for recovering an illumination distribution of a scene from image brightness observed on a real object surface. In a natural illumination condition, it is hard to recover an illumination distribution from image brightness observed on a real object surface. The main reason for this difficulty is that there is usually not adequate variation in the image brightness observed on the surface to reflect the subtle characteristics of the entire illumination.

One of the main contributions of our work is to demonstrate the effectiveness of using occluding information of incoming light in estimating the illumination distribution of a scene. Analyzing the relationships between the image brightness and the occlusions of incoming light enabled us to reliably estimate the illumination distribution of a scene even in a complex illumination environment. In addition, the question of how to provide the reflectance properties of a surface to be used for the estimation still remains from the previously proposed methods. Since it is a common situation that reflectance properties of a surface are not known, solutions to this problem are required. Another contribution of our work is that we have combined the illumination analysis with an estimation of the reflectance properties of a surface in the scene. This makes the method applicable to the case where reflectance properties of a surface are not known, and it enlarges the variety of images to which the method can be applied.

We also introduced an adaptive sampling of the illumination distribution of a scene as a solution to the question of how we could efficiently estimate the entire illumination with a smaller number of sampling directions of the entire distribution in this paper. Using the proposed adaptive sampling framework, we were able to avoid unnecessarily dense sampling of the illumination and to estimate overall illumination more efficiently by using fewer sampling directions.

While the effectiveness of the proposed method in estimating illumination distributions of usual scenes was demonstrated in this paper, the estimation was based on the assumptions that light sources in the scene were sufficiently distant from the objects, and that there was no severe interreflection between a shadow region and an *occluding object*. The future directions of this study include extending the method for: (1) considering the interreflection between a shadow region and an *occluding object*; and (2) taking distances from the *occluding object* to light sources into account.

Appendix

The proposed method estimates radiance value of the light sources based on the variations in the computed coefficients a_i in (7); we obtain n coefficients a_i $(i = 1, 2, \cdots, n)$ per image pixel where n is the number of the light sources. For reliable estimation, it is essential that we select image pixels from a *shadow image* to maximize variation in the combinations of a_i.

In our approach, the *shadow surface* is first partitioned into clusters based on combinations of the coefficients a_i. In other words, pixels that have the same combination of a_i are clustered into the same group. Fig. 15 shows several examples of partitioning based on the coefficients a_i with pseudo colors. Here each color represents an individual class with a different combination of coefficients of the light sources, and the block region corresponds to the *occluding objects*.

After the *shadow surface* are partitioned into clusters, one pixel is selected from each of those clusters. From this clustering process, we are able to avoid selecting redundant pixels that provide the same information about the illumination of the scene. This results in significant speedup of the entire estimation process as well.
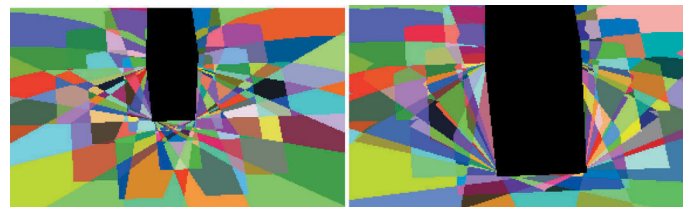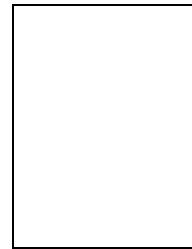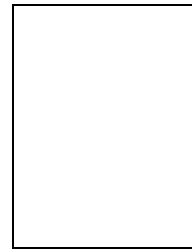

Fig. 15. Clustering results

References

[1] R. Baribeau, M. Rioux, and G. Godin, "Color Reflectance Modeling Using a Polychromatic Laser Range Sensor," *IEEE Trans. PAMI*, vol. 14, no. 2, 1992, pp. 263-269.

[2] R. Basri and D. Jacobs, "Lambertian Reflectance and Linear Subspaces," *Proc. IEEE Intl. Conf. Computer Vision 01*, 2001, pp.383-389.
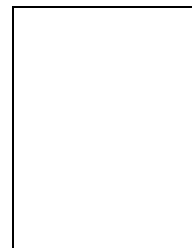
[3] J. Bouguet and P. Perona, "3D Photography on Your Desk," *Proc. IEEE Intl. Conf. Computer Vision 98*, 1998, pp.43-50.

[4] M. F. Cohen, D. P. Greenberg, D. S. Immel, and P. J. Brock, "An Efficient Radiosity Approach for Realistic Image Synthesis," *IEEE CG & A*, Vol. 6, No.3, Mar. 1986, pp.26-35.

[5] D. A. Forsyth and J. Ponce, *Computer Vision A Modern Approach*, Prentice Hall, Upper Saddle River, NJ., 2002, p. 70.

[6] A. Fournier, A. Gunawan and C. Romanzin, "Common Illumination between Real and Computer Generated Scenes,"*Proc. Graphics Interface 93*, 1993, pp.254-262.

[7] G. E. Healey, S. A. Shafer, and L. B. Wolff, *Physics-Based Vision Principles and Practice, Color*, Jones and Bartlett Publishers, Boston, MA., 1992.

[8] B. K. P. Horn,"Understanding Image Intensities," *Artificial Intelligence*, Vol. 8, No.2, 1977, pp.201-231.

[9] B. K. P. Horn, *Robot Vision*, The MIT Press, Cambridge, MA., 1986.

[10] B. K. P. Horn, "Obtaining Shape from Shading Information," *The psychology of Computer Vision*, McGraw-Hill Book Co., New York, N.Y., 1975.

[11] B. K. P. Horn and M. J. Brooks, "The Variational Approach to Shape from Shading," *Computer Vision, Graphics, and Image Processing*, Vol.33. No.2, 1986, pp.174-208.

[12] K. Ikeuchi and B. K. P. Horn, "Numerical Shape from Shading and Occluding Boundaries," *Artificial Intelligence*, Vol. 17, No.1-3, 1981, pp.141-184.

[13] K. Ikeuchi and K. Sato, "Determining Reflectance using Range and Brightness Images," *Proc. IEEE Intl. Conf. Computer Vision 90*, 1990, pp.12-20.

[14] J. Kawai, J. Painter, and M. Cohen, "Radioptimization - Boal Bawsed Rendering"*Proc. ACM SIGGRAPH 93*, 1993, pp. 147-154.

[15] G. Kay and T. Caelli, "Estimating the Parameters of an Illumination Model using Photometric Stereo,"*Graphical Models and Image Processing*, vol. 57, no. 5, 1995, pp. 365-388.

[16] J. R. Kender and E. M. Smith, "Shape from Darkness: Deriving Surface Information from Dynamic Shadows," *Proc. IEEE Intl. Conf. Computer Vision 87*, 1987, pp.539-546.

[17] T. Kim, Y. Seo, and K. Hong, "Improving AR using Shadows Arising from Natural Illumination Distribution in Video Sequence,"*Proc. IEEE Intl. Conf. Computer Vision 01*, July 2001, pp. 329-334.

[18] J. Lu and J. Little, "Reflectance Function Estimation and Shape Recovery from Image Sequence of a Rotating Object,"*Proc. IEEE Intl. Conf. Computer Vision 95*, 1995, pp. 80-86.

[19] A. K. Mackworth, *On the Interpretation of Drawings as Three-Dimensional Scenes*, doctorial dissertation, University of Sussex, 1974.

[20] S. R. Marschner and D. P. Greenberg, "Inverse Lighting for Photography," *Proc. IS&T/SID Fifth Color Imaging Conference*, 1997, pp.262-265.

[21] P. Moon and D. E. Spencer, *The Photic Field*, The MIT Press, Cambridge, MA., 1981.

[22] S. K. Nayar, K. Ikeuchi, and T. Kanade, "Surface Reflection: physical and geometrical perspectives," *IEEE Trans. PAMI*, vol. 13, no. 7, 1991, pp. 611-634.

[23] K. Nishino, Z. Zhang, and K. Ikeuchi, "Determining Reflectance Parameters and Illumination Distribution from Sparse Set of Images for View-dependent Image Synthesis," *Proc. IEEE Intl. Conf. Computer Vision 01*, Jul. 2001, pp. 599-606.

[24] A. P. Pentland, "Linear Shape From Shading," *Intl. J. Computer Vision*, Vol.4, No.2, 1990, pp.153-162.

[25] W. H. Press, B. P. Flannery, S. A. Teukolsky, W. T. Vetterling, *Numerical Recipes in C: The Art of Scientific Computing*, Cambridge University Press, Cambridge, 1988.

[26] R. Ramamoorthi and P. Hanrahan, "A Signal-Procession Framework for Inverse Rendering", *Proc. ACM SIGGRAPH 01*, Aug. 2001, pp.117-128.

[27] I. Sato, Y. Sato, and K. Ikeuchi, "Illumination Distribution from Shadows," *Proc. IEEE Conf. Computer Vision and Pattern Recognition 99*, Jun. 1999, pp. 306-312.

[28] I. Sato, Y. Sato, and K. Ikeuchi, "Illumination Distribution from Brightness in Shadows: adaptive estimation of illumination distribution with unknown reflectance properties in shadow regions," *Proc. IEEE Intl. Conf. Computer Vision 99*, Sep. 1999, pp. 875-882.

[29] I. Sato, Y. Sato, and K. Ikeuchi, "Acquiring a radiance distribution to superimpose virtual objects onto a real scene", *IEEE Trans. TVCG*, Vol. 5, No. 1, 1999, pp. 1-12.

[30] Y. Sato, M. D. Wheeler, and K. Ikeuchi, "Object shape and reflectance modeling from observation," *Proc. ACM SIGGRAPH 97*, 1997, pp. 379-387.

[31] C. Schoeneman, J. Dorsey, B. Smits, J. Arvo, and D. Greenburg, "Painting with Light,"*Proc. ACM SIGGRAPH 93*, 1993, pp. 143-146.

[32] S. A. Shafer and T. Kanade, "Using Shadows in Finding Surface Orientations," *Computer Vision, Graphics, and Image Processing*, Vol.22, 1983, No.1, pp. 145-176.

[33] S. Tominaga and N. Tanaka, "Estimating Reflectance Parameters from a Single Color Image," *IEEE Computer Graphics & Applications*, vol.20, No. 5, 2000, pp.58-66.

[34] K. E. Torrance and E. M. Sparrow, "Theory for off-specular reflection from roughened surface," *J. Optical Society of America*, vol.57, 1967, pp.1105-1114.

[35] Y. Yu, P. Devebec, J. Malik, and T. Hawkins, "Inverse Global Illumination: Recovering reflectance Models of Real Scenes from Photographs", *Proc. ACM SIGGRAPH 99*, Aug. 1999, pp.215-224.

[36] Y. Zang and Y. Yang, "Illuminant Direction Determination for Multiple Light Sources," *Proc. IEEE Conf. Computer Vision and Pattern Recognition 00*, Jun. 2000, pp. 269-276.

[37] 3D Construction Company, http://www.3dcomstruction.com

Imari Sato is a PhD student in Graduate School of Interdisciplinary Information Studies at the University of Tokyo, Tokyo, Japan. She received the BS degree in policy management from Keio University, Kanagawa, Japan, in 1994 and the MS degree in interdisciplinary information studies from the University of Tokyo in 2002. Previously, she was a visiting scholar at the Robotics Institute at Carnegie Mellon University, Pittsburgh, Pennsylvania, USA. Her research interests include physics-based vision and image-based modeling. She is a research fellow of the Japan Society for the Promotion of Science.

Yoichi Sato received the BS degree in mechanical engineering from the University of Tokyo, Tokyo, Japan, in 1990. He received the MS and PhD degrees in robotics from the School of Computer Science, Carnegie Mellon University, Pittsburgh, Pennsylvania, USA in 1993 and 1997, respectively. In 1997, he joined the Institute of Industrial Science at the University of Tokyo, where he is currently an associate professor. His primary research interests are in the fields of computer vision (physics-based vision, image-based modeling), human-computer interaction (perceptual user interface), and augmented reality. He is a member of the IEEE.

Katsushi Ikeuchi received the BEng degree in mechanical engineering from Kyoto University, Kyoto, Japan, in 1973, and the PhD degree in information engineering from the University of Tokyo, Tokyo, Japan, in 1978. He is a professor at the Institute of Industrial Science, the University of Tokyo. After working at the Artificial Intelligence Laboratory at Massachusetts Institute of Technology, the Electrotechnical Laboratory of Ministry of International Trade and Industries, and the School of Computer Science, Carnegie Mellon University, he joined the University of Tokyo in 1996. He has received various research awards, including the David Marr Prize in computational vision in 1990, and IEEE R&A K-S Fu Memorial Best Transaction Paper award in 1998. In addition, in 1992, his paper, "Numerical Shape from Shading and Occluding Boundaries," was selected as one of the most influential papers to have appeared in the Artificial Intelligence Journal within the past ten years. He is a fellow of the IEEE.